

A robust and compact representation for magnetic fields in magnetic particle imaging

G. Bringout¹ and T. M. Buzug¹

¹Institute of Medical Engineering, Universität zu Lübeck, Lübeck, Germany, {bringout,buzug}@imt.uni-luebeck.de

Abstract

In this contribution, a simple representation for magnetic fields based on spherical harmonics is presented. Compared to the acquisition on a Cartesian grid, it reduces the amount of acquired and stored data, and may increase the precision of the field representation in given scenario. The series expansion of the field generated by a drive coil is presented and the truncation error is studied. Furthermore, time and space models of the magnetic fields generated by a field-free point and a field-free line scanner using the spherical harmonic representation are presented. The proposed representation has the potential to improve the analysis of the MPI technology, by providing a compact and flexible way to represent MPI scanners and the associated magnetic fields.

1 Introduction

To date, magnetic fields used in magnetic particle imaging (MPI) scanners have mostly been defined implicitly by the coils needed to generate them or by an ideal approximation of their topology [1].

As many aspects linked to the MPI technology need to simulate, evaluate and validate the exact topology of magnetic fields, a better way to represent the fields is required. This may aim to a broader definition of the signal generation in scanners, analytical ways to design scanners, better accuracy of modeled system matrices, faster reconstruction for field-free line scanners or a technique for the quality control during the production of scanners.

An appropriate way to represent the magnetic field on a 2D- or 3D-Cartesian grid is to fit some polynomials in specific points on the grid in order to approximate the field topology. However, this technique includes two major drawbacks. First, the number of measured points may increase with the surface, volume or resolution increase, leading to a huge amount of data, which may be difficult to store and work with. Second, the approximation of the field topology with polynomials may include large errors due to an insufficient sampling and the use of fitting models with limited order [2].

The representation of divergence-free fields using series expansion overcomes those two limitations. For most coils in MPI, as the length to diameter ratio is below ten, the spherical harmonics series expansion (SHSE) is preferred. Indeed, the effects of the coil's end parts may still have a huge influence on the magnetic field topology in the center of it, and a spherical representation is better suited for this situation [2].

However, the SHSE is not exempt from drawbacks, one of them being the interpretation errors caused by the use of different normalizations. Nevertheless, this may also be advantageously used, as the different normalization may facilitate the direct evaluation of derived quantities. For example, with the Schmidt quasi-normalization, each coefficient represents the maximum amplitude reached by the corresponding spherical harmonic on a sphere, which helps to

quickly evaluate the field amplitude at different position.

In this contribution, a wide spectrum of the tools needed to understand and use this representation are presented. The SHSE is depicted in different ways, so that a correlation between the SHSE and other ways of representing magnetic fields can easily be made. To highlight the differences between the SHSE and the Cartesian representation, the magnetic field generated by a drive coil is taken as an example. Finally, theoretical field-free point (FFP) and field-free line (FFL) scanners are presented, to demonstrate the compactness and flexibility of this representation.

2 Methods

In this section the basic mathematical principles of the SHSE and its applications to the magnetic field measurement is presented.

2.1 Basic differential equation

In an investigated area, where no electric current flows, every component of a magnetic field $B_i, i = x, y, z$ satisfies the Laplace equation

$$\Delta B_i = 0 \quad (1)$$

due to Maxwell's equations [3]. To solve the Laplace equation for a given problem, some constraints have to be imposed. In the case of solving the problem with the SHSE, the Dirichlet boundary condition

$$\begin{cases} \Delta B_i = 0 & , \text{in } \{\mathbf{x} \in \mathbb{R}^3, \|\mathbf{x}\| < R\} \\ B_i(\mathbf{x}) = g(\mathbf{x}) & , \text{in } S_R^2 \end{cases} \quad (2)$$

is used. Here the values of the magnetic field components have to be known on the sphere S_R^2 with fixed radius R and are described by a continuous function g .

2.2 Solution

Applying spherical coordinates (r, θ, φ) , the solution of the problem (2) is given by the series expansion

$$B_i(r, \theta, \varphi) = \sum_{l=0}^{\infty} \sum_{m=-l}^l c_{lm}^R \left(\frac{r}{R}\right)^l Y_{lm}(\theta, \varphi), \quad (3)$$

with coefficients c_{lm}^R of the normed real spherical harmonics Y_{lm} [4]. The spherical harmonics, shown on Fig. 1, are defined by

$$Y_{lm}(\theta, \varphi) = \begin{cases} \sqrt{2} K_l^m \cos(m\varphi) P_l^m(\cos \theta) & , m > 0 \\ K_l^0 P_l^0(\cos \theta) & , m = 0 \\ \sqrt{2} K_l^{|m|} \sin(|m|\varphi) P_l^{|m|}(\cos \theta) & , m < 0 \end{cases} \quad (4)$$

with P_l^m the associated Legendre polynomials and K_l^m the normalizing factor defined by

$$K_l^m = \sqrt{\frac{(2l+1)}{4\pi} \frac{(l-m)!}{(l+m)!}}. \quad (5)$$

Here $l = 0, 1, 2, \dots$ denotes the degree and m the order of the spherical harmonic, with $-l \leq m \leq l$. The associated Legendre polynomials can be calculated using the recursion

$$\begin{aligned} P_0^0(x) &= 1 \\ P_m^m(x) &= (2m-1)!! (1-x^2)^{\frac{m}{2}} \\ P_{m+1}^m(x) &= x(2m+1)P_m^m \\ P_l^m(x) &= x \frac{2l-1}{l-m} P_{l-1}^m(x) - \frac{l+m+1}{l-m} P_{l-2}^m(x) \end{aligned} \quad (6)$$

with $0 \leq m \leq l$ and the double factorial $(2m-1)!! = \prod_{i=1}^m (2i-1)$.

2.3 Projection formula

The normalization presented in (5) forms an orthonormal basis of the square-integrable functions of the unit sphere S^2 with respect to the standard scalar product

$$\begin{aligned} \langle f, g \rangle &= \int_{S^2} fg d\Omega \\ &= \int_0^{2\pi} \int_0^\pi f(\theta, \varphi) g(\theta, \varphi) \sin(\theta) d\theta d\varphi. \end{aligned} \quad (7)$$

Thus, the coefficients c_{lm}^R from (3) can be calculated by the projection formula

$$c_{lm}^R = \int_0^{2\pi} \int_0^\pi g(\theta, \varphi) Y_{lm}(\theta, \varphi) \sin(\theta) d\theta d\varphi. \quad (8)$$

Thereby, it is sufficient to know the magnetic field on a sphere to determine the coefficients which describe the entire magnetic field of the whole ball.

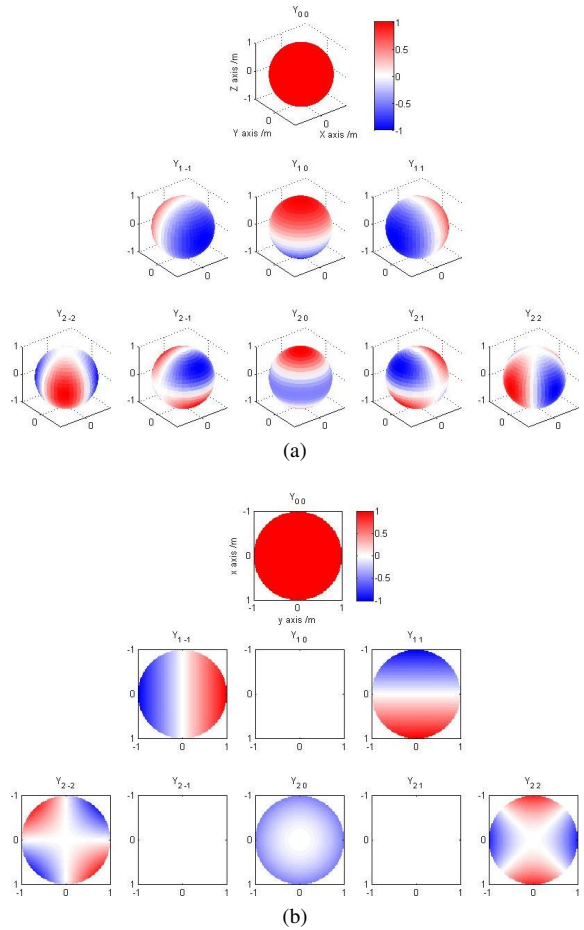


Figure 1: Two ways to represent the spherical harmonics Y_{lm} with $l \leq 2$ and $-l \leq m \leq l$. θ and φ are interpreted as spherical coordinates of the unit sphere. (a) The amplitude is represented as color variation. (b) The amplitude on the xy -plane is represented as color variation.

2.4 Normalization

Several types of normalization are commonly used, based on the wanted properties of interest. Outside the mathematical normalization presented in (5), the Schmidt quasi-normalization can also be used. It is defined as

$$K_l^m = \sqrt{\frac{(l-m)!}{(l+m)!}}, \quad (9)$$

which normalize the maximum of the spherical harmonics to one [5]. Therewith, the coefficients of the SHSE correlate immediately to the maximum influence of the corresponding spherical harmonics. However, this normalization provides no orthonormal basis and thus the projection formula (8) has to be adapted by dividing through the squared norm of the the quasi-Schmidt normalized spherical harmonic:

$$\|Y_{lm}\|^2 = \frac{4\pi}{2l+1}. \quad (10)$$

2.5 Numerical integration

A simple way to evaluate the magnetic field on a sphere is to measure its amplitude at some discrete points. In order

to do this, the integral of the projection formula (8) has to be replaced by a numerical integration formula

$$\sum_{i=1}^{N_\theta} \sum_{j=1}^{N_\varphi} \omega_i^\theta \omega_j^\varphi g(\theta_i, \varphi_j) Y_{lm}(\theta_i, \varphi_j) \sin(\theta_i) \quad (11)$$

with N_θ discretization positions of θ , N_φ discretization positions of φ and their corresponding weights ω_i^θ and ω_i^φ . Due to the independence of φ and θ in the spherical harmonics definition (4), the integral can be split into the φ -part and the θ -part.

As the φ -part contains only cosine or sine functions, the integration is done with the left rectangle method using equidistant discretization positions $\varphi_j = (j - 1) \frac{\pi}{N_\varphi}$ and the weights $\omega_j^\varphi = \frac{\pi}{N_\varphi}$.

In contrast to this, after the substitution of $s = \cos(\theta)$, the θ -part only contains the associated Legendre polynomials. Knowing that the Gaussian quadrature, also known as the Gauss-Legendre quadrature, uses weights and discretization positions determined using the Legendre polynomials, it is therefore optimal for integration of the θ -part. The N_θ discretization positions s_i are the zeros of the $N_{\theta^{\text{th}}}$ Legendre polynomial and the weights ω_i^θ are adapted in such a way, that with N_θ discretization positions a polynomial with degree $2N_\theta - 1$ can be exactly integrated [6]. The discretization of θ is therefore given by $\theta_i = \cos^{-1}(s_i)$.

2.6 Maximal order and degree

Assuming that the measured magnetic field can be completely described by spherical harmonics up to order (l_{\max}, m_{\max}) , with $l_{\max} + 1$ sampling points in θ -direction and $2m_{\max} + 1$ sampling points in φ -direction, the coefficients can be exactly computed with the proposed numerical integration formulas. This is due to the special structure of the spherical harmonics and the properties of the used numerical integration formula.

2.7 Implementation

Calculations have been done in Matlab (Matlab 7.11.0 64bit, Mathworks, Natick, USA). The implementation is available on <http://www.imt.uni-luebeck.de> and <http://github.com/gBringout/CoilDesign>.

3 Results

In this section, practical examples are given to emphasize the advantages and limitations of the SHSE for the MPI community.

3.1 Truncation error

It has been seen that a magnetic field containing a finite sum of spherical harmonics can be represented by its value on a finite number of points. But, for a given coil, it is hard to know, which spherical harmonics are included in the generated magnetic fields. Thus, it is likely that truncation errors

Table 1: Truncation error evaluation for a drive coil.

# of points	(l_{\max}, m_{\max})	$\frac{\Delta c_{00}}{c_{00}^{GS}}$	$\frac{\Delta c_{20}}{c_{20}^{GS}}$	Maximum error $\frac{\Delta c_{lm}}{c_{lm}^{GS}}$	(l, m)
45	(4,4)	0.4%	0.9%	4.6	(4,4)
66	(5,5)	0.1%	0.8%	4.3	(4,4)
6216	(55,55)	$2e^{-8}$	$6e^{-8}$	1374	(51,41)

will happen when choosing a maximal order and degree for the representation.

In order to evaluate these errors, three projections of the magnetic field generated by a coil were calculated on different sets of points and compared. The coil is shown in Fig. 2a and the results are shown in Table 1. The "gold standard" coefficient c_{lm}^{GS} were approximated by a series expansion up to degree and order 120 on 29161 points. The coefficient c_{lm} were evaluated with a series expansion up to order and degree (4,4), (5,5) and (55,55) and the absolute error was calculated as $\Delta c_{lm} = c_{lm} - c_{lm}^{GS}$.

Considering the two coefficients which have the highest amplitudes, namely c_{00} and c_{20} for the presented coil, a series expansion up to order and degree 4 is sufficient to keep the truncation error below 1 %. Even if the maximum error reach 460 % for the spherical harmonic of order 4 and degree 4, it has to be noted that the associated coefficient are here of small amplitudes, as shown in Fig. 2b.

3.2 Compactness of the representation

A field of degree $l_{\max} = 4$ and order $m_{\max} = 4$ requires only $(4 + 1) * (2 * 4 + 1) = 45$ data points per field direction to be represented. Furthermore, the storage of only 3*25 points is necessary after the usage of the projection formula (11). Those coefficient enables the reconstruction of the field anywhere in a ball of radius R with no other intrinsic resolution limitation. In comparison, a Cartesian grid as shown in Figure 2a in a 9 cm radius circle with a resolution of $2 * 2 \text{ mm}^2$ requires data on 6361 points.

3.3 Flexibility - theoretical MPI scanner

Theoretical scanners can be described by as little as thirteen factors for the case of 3D FFP scanner and fourteen for a 2D FFL scanner.

As shown in Table 2, six different SHSE coefficients linked to four different values are enough to describe the whole field topology. To provide the time variation of the fields, three frequencies have to be applied on the corresponding coefficients, knowing that the excitation is always produced via in-phased sinusoidal signal. Thus, only $6 + 4 + 3 = 13$ factors are needed to fully described a theoretical 3D FFP scanner using the SHSE.

Similarly, a 2D FFL scanner is described by nine SHSE coefficients and three related values as shown in Table 3. As for FFP scanners, sinusoidal signals are used to create the signal and spatially encode it. But, when FFP scanners use simply three sinusoidal functions, FFL scanners use amplitude modulated signals for the drive fields. Those functions

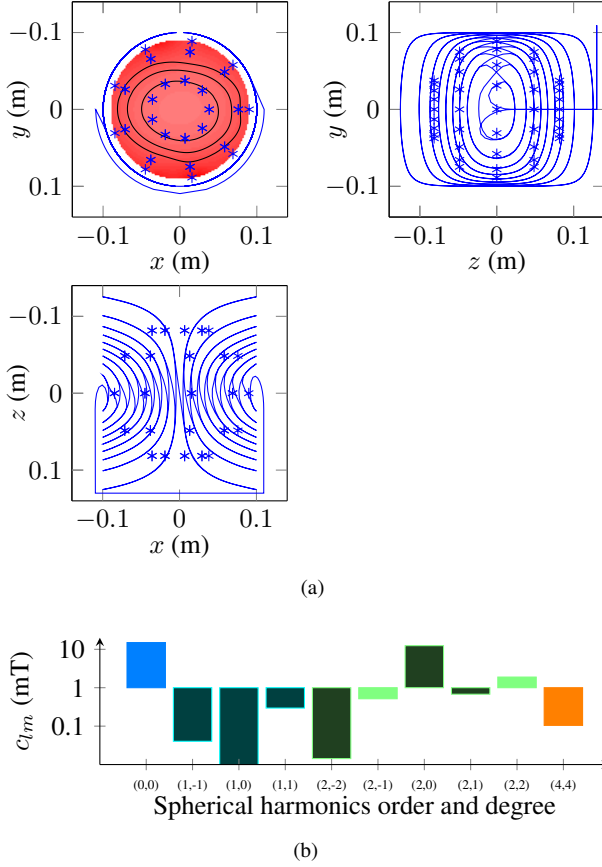


Figure 2: Representation of a drive coil with associated sampling points. (a) Front, side and top view of the model, respectively. On the front view, B_x is also represented in the xy plan. The color bar is similar to the one used in Fig 1. The contour represents the 10, 20 and 30% homogeneity limits, starting in the middle. (b) SHSE using the Schmidt quasi-normalization of the B_x fields up to the 4th degree. The first bar represents the 0th degree, the next three the 1st, etc. As a logarithmic scale is used, the negative coefficient are represented with a darker color.

are $\cos(2\pi f_1 t)$, $\sin(2\pi f_1 t)$, $\cos(\pi f_1 t) * \sin(2\pi f_2 t)$ and $\sin(\pi f_1 t) * \sin(2\pi f_2 t)$ for the Quad₀, Quad₄₅, Drive X and Drive Y generators, respectively, where t represents the time. Thus, only two frequencies are used and $9+3+2 = 14$ factors are needed to completely described a theoretical FFL scanner.

4 Conclusion

The mathematical description, compactness and flexibility of the SHSE have been presented. Using this representation, the amount of acquired and stored data for the representation of magnetic fields can be greatly reduced in comparison to the acquisition on a Cartesian grid.

Most importantly, the community can benefit from a strong and compact way to represented the time and space variation of the magnetics fields in an MPI scanners. Coupled with the description of the signal generation, this opens the way of a full scanner optimization.

Table 2: Representation of a theoretical 3D FFP scanner.

Coil's name	B_x	c_{lm}	Freq. (Hz)
Selection	$c_{11} = -a$	$c_{1-1} = a$	$c_{10} = 2a$
Drive x	$c_{00} = b$		f_1
Drive y		$c_{00} = c$	f_2
Drive z		$c_{00} = d$	f_3

Table 3: Representation of a theoretical 2D FFL scanner.

Coil's name	B_x	c_{lm}	Freq. (Hz)
Selection	$c_{11} = -a$	$c_{1-1} = a$	$c_{10} = 2a$
Quad ₀	$c_{11} = a$	$c_{1-1} = a$	f_1
Quad ₄₅	$c_{1-1} = a$	$c_{11} = a$	f_1
Drive x	$c_{00} = b$		f_1, f_2
Drive y		$c_{00} = c$	f_1, f_2

5 Acknowledgement

The authors wish to thank Alexander Weber for his contribution to the method part. The authors gratefully acknowledge the support of the German Federal Ministry of Education and Research under grant number 13N11090 as well as the European Union and the State Schleswig-Holstein with the Program for the Future-Economy under grant number 122-10-004.

References

- [1] T. M. Buzug *et al.*, “Magnetic particle imaging: Introduction to imaging and hardware realization,” *Zeitschrift für Medizinische Physik*, vol. 22, no. 4, pp. 323 – 334, 2012.
- [2] A. Wolski, “Maxwell’s equations for magnets,” in *Proceedings of the 2009 CAS-CERN Accelerator School: Specialised course on Magnets, Bruges, Belgium, 16–25 Jun 2009*, 2009, pp. 19–22.
- [3] J. D. Jackson, *Classical electrodynamics*, 3rd ed. Wiley-VCH, 1998.
- [4] G. B. Arfken and H. J. Weber, *Mathematical Methods For Physicists*, 4th ed. Academic press, 1995.
- [5] D. Winch *et al.*, “Geomagnetism and schmidt quasi-normalization,” *Geophysical Journal International*, vol. 160, no. 2, pp. 487–504, 2005.
- [6] M. Hermann, *Numerische Mathematik*. Oldenbourg Verlag, 2006.